

Enhancement of extrinsic magnetoresistance behavior in BiFeO₃ doped La_{0.8}Ag_{0.2}MnO₃ ceramic

N. Ibrahim, A.K. Yahya*

Faculty of Applied Sciences, Universiti Teknologi MARA, 40450 Shah Alam, Selangor, Malaysia

Available online 16 October 2012

Abstract

BiFeO₃ (BFO) doped La_{0.8}Ag_{0.2}MnO₃ ceramics were prepared by the conventional solid-state synthesis method to investigate the effect of BFO on transport and magnetic properties as well as its influence on magnetoresistance (MR). X-ray diffraction analysis showed a decrease in unit cell volume indicating partial substitution of some BFO into the La_{0.8}Ag_{0.2}MnO₃ (LaAgMO) lattice while results of scanning electron microscope (SEM) showed improvement in grains connectivity and formation of more regular shaped grains with BFO doping. Energy Dispersive X-ray emission (EDX) analysis showed BFO mainly segregates at the grains boundaries of LaAgMO. Resistivity and susceptibility measurements showed both metal–insulator transition temperatures, T_{MI} and paramagnetic-to-ferromagnetic transition temperature, T_c decreased with increased BFO content indicating weakening of the double exchange, DE mechanism. The temperature dependence of MR showed a small peak around T_{MI} for all samples which is ascribed to the intrinsic MR effect. Below the MR peak, the MR increased almost linearly with decreasing temperature for all samples and this is ascribed to the phenomena of extrinsic MR. The highest MR% (at 40 K) was observed for the $x=1.5\%$ sample which showed a MR of more than twice that of the undoped ($x=0\%$) sample. This extrinsic effect is suggested to be related to improved spin polarized tunneling of conduction electrons between grains under external field as a result of improved spin alignment. It is suggested that BFO induced some kind of magnetoelectric coupling between BFO and LaAgMO leading to the enhancement process.

© 2012 Elsevier Ltd and Techna Group S.r.l. All rights reserved.

Keywords: C. Electrical properties; C. Magnetic properties; Extrinsic magnetoresistance

1. Introduction

Doped-manganites with the general formula $R_{1-x}A_x\text{MnO}_3$ (R is a trivalent ion while A is a divalent or monovalent ion) have been extensively studied due to its interesting electronic and magnetic properties as well as its potential applications due to the colossal magnetoresistance (CMR) effect [1–3]. The magnetoresistance, MR which generally has a maximum value around the vicinity of metal–insulator transition temperature, T_{MI} [4] is ascribed as the intrinsic MR [4] and can be explained qualitatively by the double exchange (DE) mechanism [5] together with the Jahn–Teller effect [6].

Polycrystalline manganites also show another type of MR that is observed in a wide temperature range below T_{MI} which is ascribed as the extrinsic MR effect [4]. Spin polarized

tunneling between ferromagnetic neighboring grains [4] or spin-dependent scattering [7] is suggested to be responsible for the effect. Several groups have shown that this type of MR can be enhanced by grain boundary modifications such as doping of the divalent doped manganites with other materials as a secondary phase [7–10]. Most dopants however caused a decrease in T_{MI} . Among these, the addition of barium titanate (BTO) in divalent doped La_{0.67}Ca_{0.33}MnO₃ (LCMO) [8] showed a decrease in resistivity along with a shift of T_{MI} to higher temperatures as well as an enhanced MR. The observed behavior was suggested to be due to coupling between ferroelectric and ferromagnetic behaviors of BTO and LCMO, respectively [8]. However, studies involving ferroelectric dopants in manganites are limited while coupling effect on MR is still not fully understood.

On the other hand, BiFeO₃ (BFO) which is a multi-ferroic material displays both ferroelectric and anti-ferromagnetic properties with transition temperatures, $T_c \sim 1103$ K and $T_N \sim 643$ K, respectively [11]. It is

*Corresponding author. Tel.: +603 55444613; fax: +603 55444562.
E-mail address: ahmad191@salam.uitm.edu.my (A.K. Yahya).

interesting to investigate if doping of manganites with BFO can possibly modify properties of the CMR materials and result in enhanced extrinsic MR as the ferroelectricity (FE) of BFO may couple with the ferromagnetism of $\text{La}_{0.8}\text{Ag}_{0.2}\text{MnO}_3$. However, the effect of BFO doping on MR of CMR manganites has not been reported. Moreover, extrinsic MR has not been sufficiently studied in monovalent doped manganites.

In this work we report the effect of BFO doping on magnetotransport behavior of monovalent doped $\text{La}_{0.8}\text{Ag}_{0.2}\text{MnO}_3$ (LaAgMO) manganite. Our results showed that the introduction of BFO affects the magneto-transport behavior where low temperature MR was enhanced as a result of BFO doping. The enhanced MR at low temperatures (< 200 K) was discussed in terms of spin tunneling process at the vicinity of grain boundaries.

2. Experimental

The $(1-x)\text{La}_{0.8}\text{Ag}_{0.2}\text{MnO}_3/x\text{BiFeO}_3$ ($x=0\text{--}3.5\%$) composite samples were prepared through three different steps using

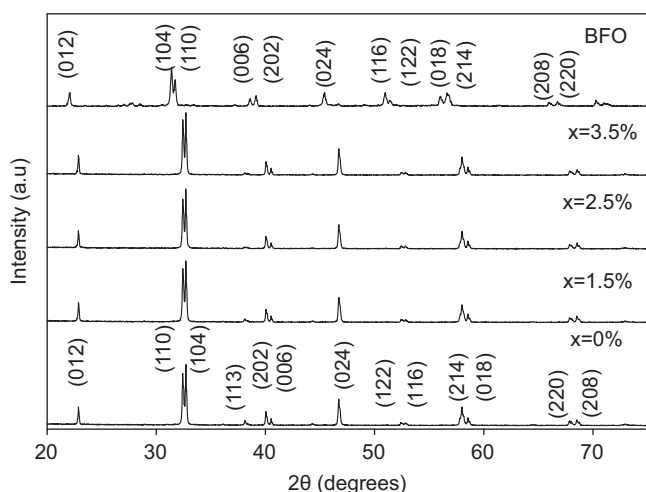


Fig. 1. XRD diffraction patterns of BFO and $(1-x)\text{La}_{0.8}\text{Ag}_{0.2}\text{MnO}_3/x\text{BFO}$ ($x=0\text{--}3.5\%$) samples.

Table 1

T_{MI} and T_{sp} at $H=0$ T, T_c , peak of MR, MR at 40 K, calculated lattice parameters, unit cell volume and best fit parameters obtained in the metallic region (at $H=0$ T) corresponding to the equation $\rho=\rho_0+\rho_2T^2$ for the $(1-x)\text{La}_{0.8}\text{Ag}_{0.2}\text{MnO}_3/x\text{BFO}$ samples.

Parameters	BFO content, x (%)			
	0	1.5	2.5	3.5
T_{MI} (K)	289	282	278	272
T_{sp} (K)	–	237	230	193
T_c (K)	285	283	282	274
Peak of MR (%)	5	8	6	5.5
MR at 40 K (%)	20	42	26	18
$a=b$ (Å)	5.533(1)	5.533(1)	5.533(1)	5.531(1)
c (Å)	13.380(2)	13.379(2)	13.374(1)	13.374(1)
V (Å ³)	354.9(2)	354.7(2)	354.6(2)	354.3(2)
ρ_0 (Ω cm)	0.097	0.028	0.061	0.141
$\rho_2 \times 10^{-6}$ (Ω cm K ⁻²)	3.714	1.294	3.519	10.53

the conventional solid state method. Firstly, $\text{La}_{0.8}\text{Ag}_{0.2}\text{MnO}_3$ (LaAgMO) were synthesized from high purity (99.99%) La_2O_3 , Ag_2O and MnO_3 oxide powders by mixing them in the appropriate stoichiometric ratio. The mixed powders were then calcined at 900 °C for 24 h with one intermediate grinding. Then, the calcinated powders was pressed into pellets and sintered at 1100 °C for 24 h. Secondly, BFO was prepared separately in the same way using high purity (99.99%) Bi_2O_3 and Fe_2O_3 oxide powders. However the calcination and sintering was done at temperatures of 800 °C and 830 °C respectively. Thirdly, appropriate amounts of the synthesized powders of LaAgMO and BFO were mixed and ground to obtain a homogeneous mixture. Finally, the mixture was pressed into pellets and sintered at 950 °C. The samples were analyzed by Philips X'Pert Pro model PW3040 X-ray diffractometer to determine the structure and phases formed. Morphology of the samples was investigated using LEO model 982 Gemini field emission scanning electron microscope (FE-SEM) and the elemental distribution was identified by energy dispersive X-ray (EDX) technique. Resistivity as a function of temperature was measured by the standard four-point probe technique under zero field and under applied magnetic field of 0.7 T. Temperature dependent AC susceptibility measurements were carried out within the temperature range of 40–300 K in an AC susceptometer system manufactured by CRYO industries, USA with its real component resolved using a 7265 DSP lock-in amplifier.

3. Results and discussion

Powder X-ray diffraction patterns of BFO and $(1-x)\text{La}_{0.8}\text{Ag}_{0.2}\text{MnO}_3/x\text{BFO}$ ($x=0\text{--}3.5\%$) are shown in Fig. 1. Analysis of XRD spectra for all samples showed all the peaks can be indexed to a rhombohedral structure with $R\bar{3}C$ space group belonging to a hexagonal setting where $a=b \neq c$. The calculated values of unit cell volume of LaAgMO (Table 1) were found to decrease as BFO content was increased. This suggests that some form of substitution took place in the LaAgMO lattice.

SEM micrograph (figure not shown) of the doped samples showed more regular and more rounded grains with increase in BFO. The EDX spectrum (figure not shown) of BFO-doped samples show existence of peaks related to Bi and Fe elements besides that of La, Ag, Mn and O. The presence of Bi and Fe at the grains supports the idea that some part of BFO may have substituted into the lattice of LaAgMnO as suggested from our XRD analyses. In addition, our EDX investigation also indicates that BFO segregates at the vicinity of the grain boundaries as well (figure not shown).

Fig. 2 shows the temperature dependence of the real (χ') part of AC susceptibility for the $(1-x)\text{La}_{0.8}\text{Ag}_{0.2}\text{MnO}_3/x\text{BFO}$ samples. The paramagnetic (PM) to ferromagnetic (FM) transition temperatures, T_c were determined based on the minimum point obtained from $d\chi'/dT$ vs. T plots such as that shown in the inset of Fig. 2. As shown in Table 1, the T_c values were found to decrease from 285 K ($x=0\%$) to 274 K ($x=3.5\%$).

Fig. 3 shows the resistivity vs. temperature plot for $(1-x)\text{La}_{0.8}\text{Ag}_{0.2}\text{MnO}_3/x\text{BFO}$ ($x=0-3.5\%$) samples in zero magnetic field. The metal–insulator transition temperature, T_{MI} was found to decrease from 289 K ($x=0\%$) to 272 K ($x=3.5\%$). The observed decrease in both T_{MI} and T_c values

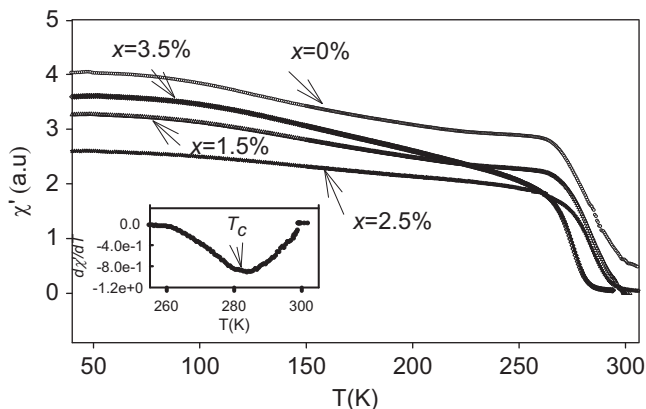


Fig. 2. Temperature dependence of the real (χ') part of AC susceptibility of $(1-x)\text{La}_{0.8}\text{Ag}_{0.2}\text{MnO}_3/x\text{BFO}$ samples.

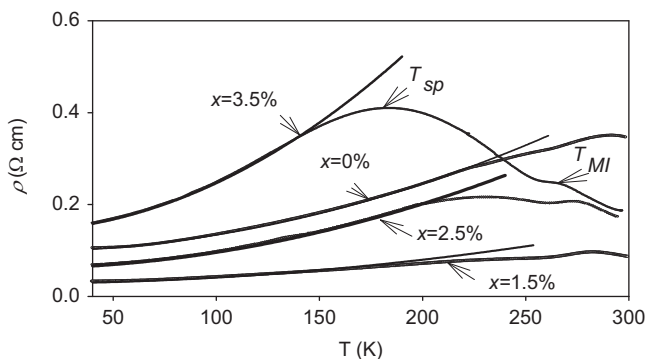


Fig. 3. The resistivity vs. temperature curve of the $(1-x)\text{La}_{0.8}\text{Ag}_{0.2}\text{MnO}_3/x\text{BFO}$ samples ($x=0-3.5\%$) in a zero magnetic field. The solid lines gives the best fitting using the equation $\rho = \rho_0 + \rho_2 T^2$.

as BFO content was increased is due to weakening of the DE mechanism as a result of the partial substitution of BFO into the lattice as indicated by XRD and EDX analyses. The resistivity of the samples in the whole temperature region was found to decrease at $x=1.5\%$ before increasing back for $x=2.5\%$ and $x=3.5\%$. Besides that, the resistivity vs. temperature curves (Fig. 3) for BFO doped samples exhibit a secondary peak at T_{sp} , which occurred at slightly lower temperatures than that of T_{MI} with the enhanced secondary peak clearly observed for $x=3.5\%$. The observed peak indicates that an insulating phase may be involved, which could be attributed to inhomogeneity [2,3,7]. Since the secondary peak is a maximum resistivity which coincides with the FM region, the inhomogeneity may be in the form of ferromagnetic insulating, FMI phase which increases with BFO doping within the larger and dominant FMM matrix. The existence of FMI phase among FMM phase may lead to disconnected FMM phase [3] and hence affects the DE mechanism which caused the increase in resistivity at the vicinity of T_{sp} .

The experimental zero-field resistivity data have been fitted with the empirical equations representing different scattering mechanisms as given in Refs. [2,3]. The best fit, with the square of linear correlation coefficient (R^2) as high as 99.99%, was found for the scattering equation $\rho = \rho_0 + \rho_2 T^2$ for all samples. In the equation, ρ_0 is the resistivity due to grain boundary effects and ρ_2 is the resistivity contributed by electron–electron scattering process [2,3].

The fitting parameters, ρ_0 and ρ_2 were found to be smaller for $x=1.5\%$ and $x=2.5\%$ samples (Table 1) compared to undoped sample indicating that BFO doping may have reduced the scattering of conduction electrons and hence lowered the resistivity of the samples (Fig. 3). However, the increase in both ρ_0 and ρ_2 values for $x=3.5\%$ could be attributed to an enhancement of grain boundary contribution which results in the increase in electron–electron scattering.

The temperature dependence of MR for all samples is presented in Fig. 4 where MR (%) was calculated using the equation, $\text{MR}(\%) = [\rho(0, T) - \rho(H, T) / \rho(0, T)] \times 100\%$, where $\rho(0, T)$ and $\rho(H, T)$ are the resistivities under external magnetic field of $H=0$ T and $H=0.7$ T respectively [2]. The MR (%) for all the samples were found to increase

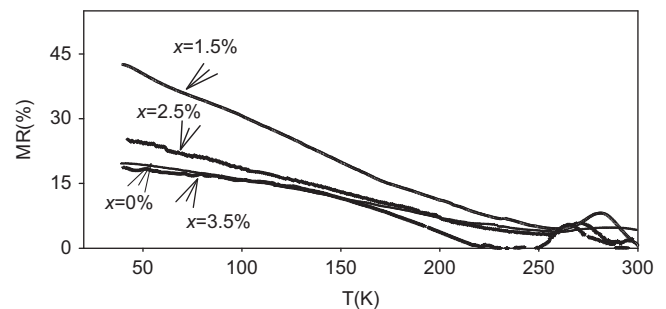


Fig. 4. The temperature dependence of MR for $(1-x)\text{La}_{0.8}\text{Ag}_{0.2}\text{MnO}_3/x\text{BFO}$ samples.

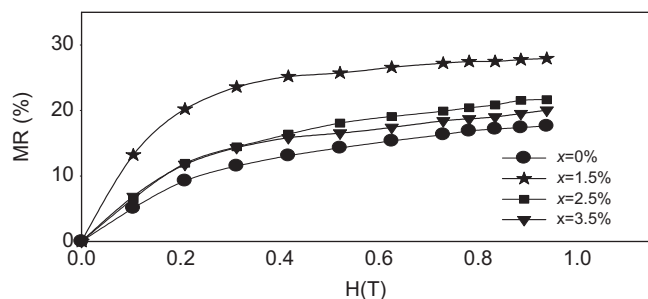


Fig. 5. The magnetic field dependence of MR for $(1-x)\text{La}_{0.8}\text{Ag}_{0.2}\text{MnO}_3/x\text{BFO}$ samples at 40 K.

almost linearly with decreasing temperature below 200 K; and there was a small peak at the vicinity of T_{MI} which was due to intrinsic MR as a result of the DE interaction [7]. The variation of MR peak height (Table 1) indicates some small influence of BFO on intrinsic MR. On the other hand, below 200 K, for instance at 40 K (Table 1), the MR was found to be much larger in BFO-doped samples $x=1.5\%$ and $x=2.5\%$ indicating that the MR is obviously enhanced by the BFO doping. The observed increase in MR below 200 K (Fig. 4) for $x=1.5\%$ and $x=2.5\%$ may be due to extrinsic MR which is related to the enhancement of spin polarized tunneling effect between grains. This could also be related to suppression of spin disorder as a result of applied magnetic field which modified magnetization between grains [7,10]. The increased MR may also be attributed to the grain boundaries acting as thin barriers which accordingly weakened electron scattering and facilitates spin polarized tunneling between grains [7]. The weakening of electron scattering at the barrier may be due to some form of magnetoelectric, ME coupling effect associated with the ferroelectric property of BFO and the ferromagnetic DE mechanism in LaAgMO . Similar coupling has been suggested by Ren et al. [8] in BTO-doped LCMO. However, the observed reduction of the extrinsic MR at $x=3.5\%$ indicates that excess doping caused large scattering effect which weakened the spin alignment under external field and reduced the tunneling process.

Fig. 5 shows the field dependence of MR at 40 K for all samples. The MR was found to increase sharply at low field ($H < 0.3$ T) with larger slope observed for $x=1.5\%$. The large increase in extrinsic MR produced by the tunneling process may have caused the observed sharp increase in MR [9]. Application of a small magnetic field at low temperatures is likely to produce strong magnetization effect between grains for $x=1.5\%$. This indicates that the extrinsic MR and magnetic field sensitivity ($d\text{MR}/dH$) can be enhanced by the low BFO doping. The results also suggest that the tunneling phenomenon occurs dominantly at low temperatures region [4,9] and was responsible for the low field MR. On the other hand, the MR of all samples increased almost linearly with lower slope at magnetic fields of larger than 0.3 T and this effect was

could be related to magnetic field induced magnetic ordering at the surface or grain boundaries [10].

4. Conclusion

In summary, effects of BiFeO_3 doping on transport and magnetic properties of $(1-x)\text{La}_{0.8}\text{Ag}_{0.2}\text{MnO}_3/x\text{BFO}$ composites were investigated. The decrease of T_{MI} and T_C with BFO doping is suggested to be due to weakening of the double exchange mechanism as a result of partial substitution of BFO into the LaAgMO lattice as indicated by XRD analyses. On the other hand, part of the BFO segregated at the grain boundaries of LaAgMO contributed to increase in magnetic inhomogeneity. The enhanced MR at low temperature region (< 200 K) for $x=1.5\%$ and $x=2.5\%$ could be related to enhancement of spin polarized tunneling process between grains. However, the decrease in MR for $x=3.5\%$ may be due to the increase in magnetic inhomogeneity which reduced the rate of the tunneling process. The behavior in both temperature dependent MR and magnetic field dependent MR suggests that the tunneling phenomenon is dominant at low temperatures.

References

- [1] S. Jin, T.H. Tiefel, M. Mc Cormack, R.A. Fastnacht, R. Ramesh, L.H. Chen, Thousandfold change in resistivity in magnetoresistive La-Ca-Mn-O films, *Science* 264 (1994) 413–415.
- [2] Y. Kalyana Lakshmi, P. Venugopal Reddy, Electrical behavior of some silver-doped lanthanum-based CMR materials, *Journal of Alloys and Compounds* 470 (2009) 67–74.
- [3] M. Battabyal, T.K. Dey, Electrical conductivity in $\text{La}_{1-x}\text{Ag}_x\text{MnO}_3$ pellets between 10 and 350 K, *Physica B* 367 (2005) 40–47.
- [4] H.Y. Hwang, S.W. Cheong, N.P. Ong, B. Batlogg, Spin polarized intergrains tunneling in $\text{La}_{2/3}\text{Sr}_{1/3}\text{MnO}_3$, *Physical Review Letters* 77 (1996) 2041–2044.
- [5] C. Zener, Interaction between the d-shells in the transition metals. II. Ferromagnetic compounds of manganese with perovskite structure, *Physical Review B* 82 (1951) 403–405.
- [6] A.J. Millis, B.I. Shraiman, R. Muller, Dynamic Jahn–Teller, effect and colossal magnetoresistance in $\text{La}_{1-x}\text{Sr}_x\text{MnO}_3$, *Physical Review Letters* 77 (1996) 175–178.
- [7] C.S. Xiong, F.F. Wei, Y.H. Xiong, L.J. Li, Z.M. Ren, X.C. Bao, Y. Zheng, Y.B. Pi, Y.P. Zhou, X. Wu, C.F. Zheng, Electrical properties and magnetoelectric effect measurement in $\text{La}_{0.7}\text{Ca}_{0.2}\text{Sr}_{0.1}\text{MnO}_3/x\text{CoFe}_2\text{O}_3$ composites, *Journal of Alloys and Compounds* 474 (2009) 316–320.
- [8] G.M. Ren, S.L. Yuan, H.G. Guan, X. Xiao, G.Q. Yu, J.H. Miao, Y.Q. Wang, S.Y. Yin, Electrical transport and magnetoresistance in $\text{La}_{0.67}\text{Ca}_{0.33}\text{MnO}_3/\text{BaTiO}_3$ composites, *Materials Letters* 39 (2007) 767–769.
- [9] A. Gaur, G.D. Varma, Low field magnetoresistance in $\text{La}_{0.67}\text{Ca}_{0.33}\text{MnO}_3$ and Co_3O_4 combined system, *Journal of Alloys and Compounds* 453 (2008) 423–427.
- [10] B. Huang, Y.-H. Liu, X. Yuan, C. Wang, R.-Z. Zhang, L. Mei, The unusual magnetotransport properties of $\text{La}_{0.67}\text{Sr}_{0.33}\text{MnO}_3$ with Nb_2O_5 addition, *Journal of Magnetism and Magnetic Materials* 280 (2004) 176–183.
- [11] A.K. Pradhan, K. Zhang, D. Hunter, J.B. Dadson, G.B. Loutts, P. Bhattacharya, R. Katiyar, J. Zhang, D.J. Sellmyer, U.N. Roy, Y. Cui, A. Burger, Magnetic and electrical properties of single-phase BiFeO_3 , *Journal of Applied Physics* 97 (2005) 092903-1-4.